Spectral Domain Immitance Approach for Dispersion Characteristics of Generalized Printed Transmission Lines

TATSUO ITOH, SENIOR MEMBER, IEEE

Abstract—**A simple method for formulating the dyadic Green's functions in the spectral domain is presented for generalized printed transmission lines which contain several dielectric layers and conductors appearing at several dielectric interfaces. The method is based on the transverse equivalent transmission line for a spectral wave and on a simple coordinate transformation. This formulation process is so simple that often it is accomplished almost by inspection of the physical cross-sectional structure of the transmission line. The method is applied to a new versatile transmission line, a microstrip-slot line, and some numerical results are presented.**

I. Introduction

A FEW YEARS AGO, a method called the spectral-domain technique was developed for efficient numerical analyses for various planar transmission lines and successfully applied to a number of structures [1], [2]. One difficulty in applying this technique is that a lengthy derivation process is required in the formulation stage, especially for the more complicated structures such as the one recently proposed by Aikawa [3], [4] in which more than one conductor are located at different dielectric interfaces. This paper presents a simple method for deriving the dyadic Green's functions (immittance functions) which is based on the transverse equivalent circuit concept as applied in the spectral domain in conjunction with a simple coordinate transformation rule. This technique is quite versatile and the formulation of the Green's function may be done almost by inspection in many structures. It is noted that symmetry in the structure is not required and that the analysis can be extended to finite circuit elements, such as the disk resonator.

In what follows, we first illustrate the formulation process for the microstrip line and subsequently extend it to a more general microstrip-slot structure. Numerical results for the microstrip-slot structure are also presented.

II. Illustration of the Formulation Process

To illustrate the formulation process, we will use a simple shielded microstrip line shown in Fig. 1. In conventional space-domain analysis [5], this structure may be analyzed by first formulating the following coupled homogeneous integral equations and then solving for the unknown propagation constant β:

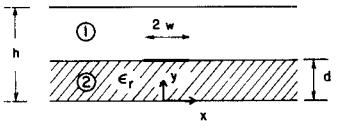

Fig. 1. Cross section of a microstrip line.

$$\int [Z_{zz}(x-x',d)J_z(x')+Z_{zx}(x-x',d)J_x(x')]\,dx'=0 \tag{1}$$

$$\int [Z_{xz}(x-x',d)J_z(x')+Z_{xx}(x-x',d)J_x(x')]\,dx=0 \tag{2}$$

where J_x and J_z are unknown current components on the strip and the Green's functions (impedance functions) Z_{zz}, etc., are functions of unknown β as well. The integration is over the strip, and (1) and (2) are valid on the strip. The left-hand sides of these equations give E_z and E_x components on the strip and, hence, are required to be zero to satisfy the boundary condition at the perfectly conducting strip. These equations may be solved provided that Z_{zz}, etc., are given. However, for the inhomogeneous structures, these quantities are not available in closed forms.

In the spectral domain formulation, we use Fourier transforms of (1) and (2) and deal with algebraic equations

$$\tilde{Z}_{zz}(\alpha,d)\tilde{J}_z(\alpha,d)+Z_{zx}(\alpha,d)\tilde{J}_x(\alpha,d)=\tilde{E}_z(\alpha,d) \tag{3}$$

$$\tilde{Z}_{xz}(\alpha,d)\tilde{J}_z(\alpha,d)+Z_{xx}(\alpha,d)\tilde{J}_x(\alpha,d)=\tilde{E}_x(\alpha,d) \tag{4}$$

instead of the convolution-type coupled integral equations (1) and (2). In (3) and (4), quantities with $\sim$ are Fourier transforms of corresponding quantities without $\sim$. The Fourier transform is defined as

$$\tilde{\phi}(\alpha)=\int_{-\infty}^{\infty}\phi(x)e^{j\alpha x}\,dx. \tag{5}$$

Notice that the right-hand sides of (3) and (4) are no longer zero because they are the Fourier transforms of E_z and E_x on the substrate surface which are obviously nonzero except on the strip. Hence, algebraic equations (3) and (4) contain four unknowns $\tilde{J}_z$, $\tilde{J}_x$, $\tilde{E}_z$, and $\tilde{E}_x$. However, $\tilde{E}_z$ and $\tilde{E}_x$ will be eliminated later in the solution process based on the Galerkin's procedure.

Manuscript received October 26, 1979; revised February 2, 1980. This work was supported in part by U.S. Army Research Office under Grant DAA29-78-G-0145.

The author is with the Department of Electrical Engineering, University of Texas, Austin, TX 78712.

0018-9480/80/0700-0733$00.75 ©1980 IEEE

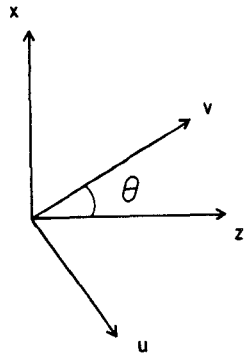

Fig. 2. Coordinate transformation.

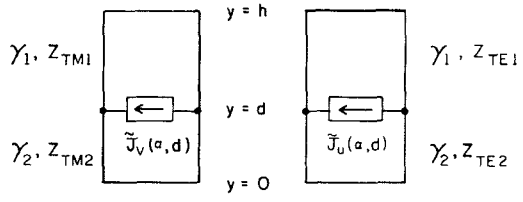

Fig. 3. Equivalent transmission lines for the microstrip line.

The closed forms of Green's impedance functions $\tilde{Z}_{zz}$, etc., can be derived by first writing the Fourier transforms of field components in each region in terms of superposition of TM-to-y and TE-to-y expressions by way of Maxwell's equations.

$$\begin{aligned}\tilde{E}_y(\alpha,y) &= A^e \cosh\gamma_1 y, && 0<y<d\\ &= B^e \cosh\gamma_2(h-y), && d<y<h \end{aligned} \tag{6}$$

$$\begin{aligned}\tilde{H}_y(\alpha,y) &= A^h \sinh\gamma_1 y, && 0<y<d\\ &= B^h \sinh\gamma_2(h-y), && d<y<h \end{aligned} \tag{7}$$

$$\gamma_1=\sqrt{\alpha^2+\beta^2-\epsilon_r k^2} \qquad \gamma_2=\sqrt{\alpha^2+\beta^2-k^2}\,. \tag{8}$$

Next, we match tangential (x and z) components at the interface and apply appropriate boundary conditions at the strip [1], [2]. By eliminating A^e, B^e, A^h, and B^h from these conditions, we obtain expressions for Green's impedance functions $\tilde{Z}_{zz}$, etc.

In the new formulation process we will make use of equivalent transmission lines in the y direction. To this end, we recognize that from

$$E_y(x,y)e^{-j\beta z}=\frac{1}{2\pi}\int_{-\infty}^{\infty} E_y(\alpha,y)e^{-j(\alpha x+\beta z)}d\alpha \tag{9}$$

all the field components are a superposition of inhomogeneous (in y) waves propagating in the direction of θ from the z axis where $\theta=\cos^{-1}(\beta/\xi)$, $\xi=\sqrt{\alpha^2+\beta^2}$. For each θ, waves may be decomposed into TM-to-y ($\tilde{E}_y,\tilde{E}_v,\tilde{H}_u$), and TE-to-$y$ ($\tilde{H}_y,\tilde{E}_u,\tilde{H}_v$) where the coordinates v and u are as shown in Fig. 2 and related with (x,z) via

$$\begin{aligned} u &= z\sin\theta - x\cos\theta\\ v &= z\cos\theta + x\sin\theta. \end{aligned} \tag{10}$$

We recognize that $\tilde{J}_v$ current creates only the TM fields and $\tilde{J}_u$ the TE fields. Hence, we can draw equivalent circuits for the TM and TE fields as in Fig. 3. The characteristic admittances in each region are

$$Y_{\mathrm{TM}i}=\frac{\tilde{H}_u}{\tilde{E}_v}=\frac{j\omega\epsilon_0\epsilon_i}{\gamma_i}, \qquad i=1,2 \tag{11}$$

$$Y_{\mathrm{TE}i}=-\frac{\tilde{H}_v}{\tilde{E}_u}=\frac{\gamma_i}{j\omega\mu}, \qquad i=1,2 \tag{12}$$

where $\gamma_i=\sqrt{\alpha^2+\beta^2-\epsilon_i k^2}$ is the propagation constant in the y direction in the ith region. All the boundary conditions for the TE and TM waves are incorporated in the equivalent circuits. For instance, the ground planes at $y=0$ and h are represented by short circuits at respective places. The electric fields $\tilde{E}_v$ and $\tilde{E}_u$ are continuous at $y=d$ and are related to the currents via

$$\tilde{E}_v(\alpha,d)=\tilde{Z}^e(\alpha,d)\tilde{J}_v(\alpha,d) \tag{13}$$

$$\tilde{E}_u(\alpha,d)=\tilde{Z}^h(\alpha,d)\tilde{J}_u(\alpha,d). \tag{14}$$

$\tilde{Z}^e$ and $\tilde{Z}^h$ are the input impedances looking into the equivalent circuits at $y=d$ and are given by

$$\tilde{Z}^e(\alpha,d)=\frac{1}{Y_1^e+Y_2^e} \tag{15}$$

$$\tilde{Z}^h(\alpha,d)=\frac{1}{Y_1^h+Y_2^h} \tag{16}$$

where Y_1^e and Y_2^e are input admittances looking down and up at $y=d$ in the TM equivalent circuit and Y_1^h and Y_2^h are those in the TE circuit:

$$Y_1^e=Y_{\mathrm{TM}1}\coth\gamma_1(h-d) \qquad Y_2^e=Y_{\mathrm{TM}2}\coth\gamma_2 d \tag{17}$$

$$Y_1^h=Y_{\mathrm{TE}1}\coth\gamma_1(h-d) \qquad Y_2^h=Y_{\mathrm{TE}2}\coth\gamma_2 d. \tag{18}$$

The final step consists of the mapping from the (u,v) to (x,z) a coordinate system for the spectral wave corresponding to each θ given by α and β. Because of the coordinate transform (10), E_x and E_z are linear combinations of E_u and E_v. Similarly, J_x and J_z are superpositions of J_u and J_v. When these relations are used, the impedance matrix elements in (3) and (4) are found to be

$$\tilde{Z}_{zz}(\alpha,d)=N_z^2\tilde{Z}^e(\alpha,d)+N_x^2\tilde{Z}^h(\alpha,d) \tag{19}$$

$$\tilde{Z}_{zx}(\alpha,h)=\tilde{Z}_{xz}(\alpha,d)=N_xN_z\left[-\tilde{Z}^e(\alpha,d)+\tilde{Z}^h(\alpha,d)\right] \tag{20}$$

$$\tilde{Z}_{xx}(\alpha,d)=N_x^2\tilde{Z}^e(\alpha,d)+N_z^2\tilde{Z}^h(\alpha,d) \tag{21}$$

where

$$N_x=\frac{\alpha}{\sqrt{\alpha^2+\beta^2}}=\sin\theta \qquad N_z=\frac{\beta}{\sqrt{\alpha^2+\beta^2}}=\cos\theta. \tag{22}$$

Notice that $\tilde{Z}^e$ and $\tilde{Z}^h$ are functions of $\alpha^2+\beta^2$ and the ratio of α to β enters only through N_x and N_z.

It is easily shown that (19)–(21) are identical to those previously derived by means of boundary value problems imposed on the field expression [1], [2].

III. Extension to the Microstrip-Slot Structure

The method presented in the previous section may be extended to more complicated structures such as the microstrip-slot line structure in Fig. 4. This structure is

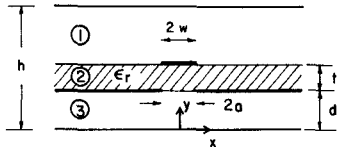

Fig. 4. Cross section of a microstrip-slot line.

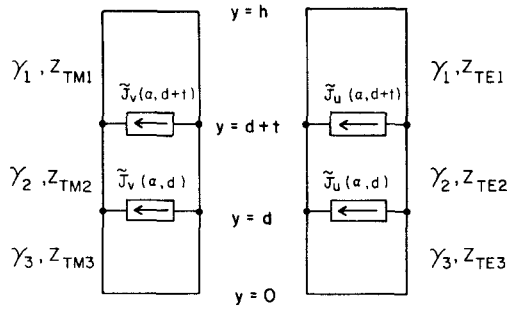

Fig. 5. Equivalent transmission lines for the microstrip-slot line.

believed to be useful in many microwave integrated circuit designs because there is an additional degree of freedom in design due to the existence of the slot [3], [4], [6]. The characteristic impedance and the propagation constant may be altered from those in the microstrip line by changing the slot width in the new structure.

By comparing the new structure with the microstrip line in Fig. 1, we may draw equivalent circuits in Fig. 5. From Fig. 5, we get

$$\tilde{E}_v(\alpha, d+t) = \tilde{Z}^e_{11}\tilde{J}_v(\alpha, d+t) + \tilde{Z}^e_{12}\tilde{J}_v(\alpha, d) \quad (23a)$$

$$\tilde{E}_u(\alpha, d+t) = \tilde{Z}_{11}\tilde{J}_u(\alpha, d+t) + \tilde{Z}^h_{12}\tilde{J}_u(\alpha, d) \quad (23b)$$

$$\tilde{E}_v(\alpha, d) = \tilde{Z}^e_{21}\tilde{J}_v(\alpha, d+t) + \tilde{Z}^e_{22}J_v(\alpha, d) \quad (24a)$$

$$\tilde{E}_u(\alpha, d) = \tilde{Z}^h_{21}\tilde{J}_u(\alpha, d+t) + \tilde{Z}_{22}\tilde{J}_u(\alpha, d) \quad (24b)$$

where $\tilde{Z}^e_{11}$ is the driving point input impedance at $y = d+t$ and $\tilde{Z}_{12}$ is the transfer impedance which expresses the contribution of the source at $y = d$ to the field at $y = d+t$. Other quantities may be similarly defined. Specifically

$$Z^e_{11} = \frac{1}{Y^e_1 + Y^e_{2L}} \quad (25)$$

$$Y^e_1 = Y_{TM1}\coth\gamma_1(h-d-t) \quad (26)$$

$$Y^e_{2L} = Y_{TM2}\frac{Y_{TM2} + Y^e_3\coth\gamma_2 t}{Y^e_3 + Y_{TM2}\coth\gamma_2 t} \quad (27)$$

where

$$Y^e_3 = Y_{TM3}\coth\gamma_3 d. \quad (28)$$

It is readily seen that Y^e_3 and Y^e_{2L} are input impedances looking down at $y = d$ and $d+t$, respectively, while Y^e_1 is the one looking upward at $y = d+t$. On the other hand

$$\tilde{Z}^e_{12} = \frac{1}{Y^e_3 + Y^e_{2u}}\frac{Y_{TM2}/\sinh\gamma_2 t}{Y^e_1 + Y_{TM2}\coth\gamma_2 t}. \quad (29)$$

Here

$$Y^e_{2u} = Y_{TM2}\frac{Y_{TM2} + Y^e_1\coth\gamma_2 t}{Y^e_1 + Y_{TM2}\coth\gamma_2 t}$$

is the input admittance looking upward at $y = d$. We recognize that Z^e_{12} is the transfer impedance from Port 2 to Port 1 in the TM equivalent circuit. All other impedance coefficients in (23) and (24) may be similarly derived.

Impedance-matrix elements may be derived by the coordinate transform identical to the one used in the microstrip case. Some of the results are

$$\tilde{Z}^{11}_{zz} = N_z^2\tilde{Z}^e_{11} + N_x^2\tilde{Z}^h_{11} \quad (30)$$

$$\tilde{Z}^{11}_{zx} = N_zN_x(-\tilde{Z}^e_{11} + \tilde{Z}^h_{11}) \quad (31)$$

$$\tilde{Z}^{12}_{zz} = N_z^2\tilde{Z}^e_{12} + N_x^2\tilde{Z}^h_{12}. \quad (32)$$

The subscripts, say zx, indicate the direction of the field (E_z) caused by that of the contributing current (J_x). The superscripts, say 12, signify the relation between the interface where the field is observed (1) and the one where the current is present (2).

IV. Some Features of the Method

The method presented here is useful in solving many printed line problems. We will summarize the procedure for the formulation. 1) When the structure is given, we first draw TM and TE equivalent circuits. Each layer of dielectric medium is represented by different transmission lines and whenever conductors are present at particular interfaces, we place current sources at the junctions between transmission lines. At the ground planes, these transmission lines are shorted. 2) We derive driving point and transfer impedances from the equivalent circuits. 3) They are subsequently combined according to the sub- and superscript conventions described in the previous section, and we obtain the necessary impedance matrix elements.

The method has certain attractive features:

1) When the structures are modified, such changes are easily accommodated. For instance, when our structure has sidewalls, at say $x = \pm L$, to completely enclose the printed lines, all the procedures remain unchanged provided the discrete Fourier transform is used

$$\tilde{\phi}(\alpha) = \int_{-L}^{L}\phi(x)e^{j\alpha x}dx, \qquad \alpha = \frac{n\pi}{2L}. \quad (33)$$

On the other hand, when the top wall is removed, we only replace the shorted transmission line for the top-most layer with a semi-infinitely long one extending to $y \to +\infty$.

2) The formulation is independent of the number of strips and their relative location at each interface. Information on these parameters is used in the Galerkin's procedure to solve equations such as (3) and (4).

3) For some structures such as fin lines [8], it is more advantageous to use admittance matrix which provides the current on the fins due to the slot field. The formulation in this case almost parallels the present one. Instead of the current sources, we need to use voltage sources in the equivalent circuits.

4) It is easily shown that the method is applicable to finite structures such as microstrip resonators and antennas. Instead of (5), we need to use double Fourier transforms in x and z directions so that only the y dependence remains to allow the use of equivalent circuit concept.

5) Certain physical information is readily extracted. For instance, it is clear that denominators of typical impedance matrix elements give the transverse resonance equation when equated to zero. This implies that for certain spectral waves determined by α and β, surface wave poles may be encountered. How strongly the surface wave is excited, or if it is excited at all, is determined by the structure.

V. Numerical Example

Although the intention of this paper is to show the formulation process, the additional steps required to obtain numerical results are discussed for the sake of completeness. We computed dispersion characteristics of the microstrip-slot line with sidewalls at $x=\pm L$ by the present formulation followed by a Galerkin's procedure repeatedly used in the spectral-domain method.

In the previous section, the problem is formulated by using the impedance matrix with elements Z_{pq}^{ij}, $(i,j=1,2$ and $p,q=x,z)$ and we presumed that the current components on the conductors are unknown. It is more advantageous in numerical calculation if we choose the current components on the strip $\tilde{J}_z(\alpha,d+t)$ and $\tilde{J}_x(\alpha,d+t)$ and the aperture fields in the slot $\tilde{E}_z(\alpha,d)$ and $\tilde{E}_x(\alpha,d)$ for unknowns in the Galerkin's procedure. This is because the aperture field in the slot can be more accurately approximated than the current on the conductor at $y=d$ [4], [7]. To this end, we rearrange the impedance matrix equation to the one in which the above four unknown quantities are on the left-hand side. This modification can be readily accomplished. In the Galerkin's method, these unknowns are expressed in terms of known basis functions. Finally, we obtain homogeneous linear simultaneous equations as the right-hand side becomes identically zero by the inner product process [1], [2]. By equating the determinant to zero, we find the eigenvalue β.

There are two types of modes in the structure. One of them is a perturbed microstrip mode and another is a perturbed slot mode. For the perturbed microstrip quasi-TEM mode, we have computed dispersion relations by choosing only one basis function each for four unknowns. They are chosen such that appropriate edge conditions are satisfied at the edges of strip and slot. For instance, we can choose as the basis functions the Fourier transforms of

$$J_z(x,d+t)=\frac{1}{\sqrt{w^2-x^2}} \qquad J_x(x,d+t)=x\sqrt{w^2-x^2}$$

$$E_z(x,d)=\sqrt{a^2-x^2} \qquad E_x(x,d)=\frac{x}{\sqrt{a^2-x^2}}.$$

It is readily seen that Fourier transforms of these functions are analytically given in terms of Bessel functions. Fig. 6 shows some numerical examples of dispersion characteristics. The present results for a small slot width are compared with those of a shielded microstrip line [1]. It is clear that as the frequency increases, the presence of nonzero slot width becomes more significant. It is also seen that, as the slot width increases, the guide wavelength becomes larger because the effect for the free space below the slot is more pronounced. This suggests that the guide wavelength is adjustable by two means, one by changing the strip width and another by varying the slot width.

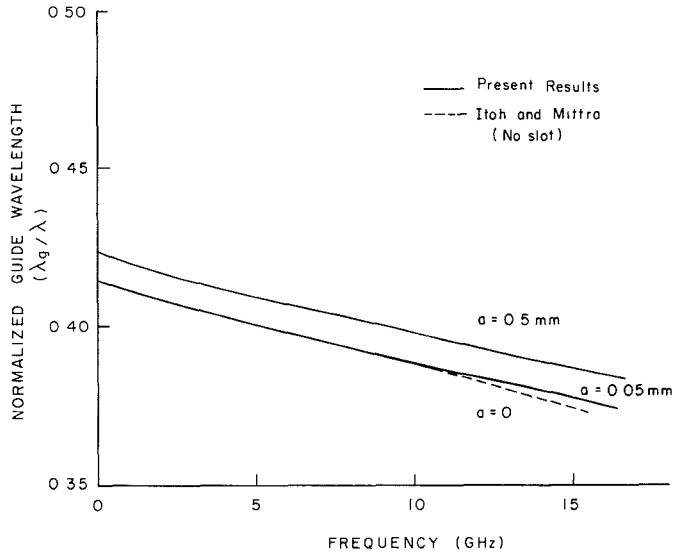

Fig. 6. Dispersion characteristics of microstrip-slot lines $L=6.35$ mm, $d=11.43$ mm, $t=1.27$ mm, $h=24.13$ mm, $w=0.635$ mm, $\epsilon_r=8.875$.

VI. Conclusions

We presented a simple method for formulating the eigenvalue problems for dispersion characteristics of general printed transmission lines. The method is intended to save considerable analytical labor for these types of problems. In addition, the method provides certain unique features. The method is applied to the problem of microstrip-slot line believed useful in microwave- and millimeter-wave integrated circuits. Numerical results are also presented.

References

[1] T. Itoh and R. Mittra, "A technique for computing dispersion characteristics of shielded microstrip lines," *IEEE Trans. Microwave Theory Tech.*, vol. MTT-22, pp. 896–898, Oct. 1974.

[2] T. Itoh, "Analysis of microstrip resonators," *IEEE Trans. Microwave Theory Tech.*, vol. MTT-22, pp. 946–952, Nov. 1974.

[3] M. Aikawa, "Microstrip line directional coupler with tight coupling and high directivity," *Electron. Commun. Jap.*, vol. J60-B, pp. 253–259, Apr. 1977.

[4] H. Ogawa and M. Aikawa, "Analysis of coupled microstrip-slot lines," *Electron. Commun. Jap.*, vol. J62-B, pp. 396–403, Apr. 1979.

[5] G. I. Zysman and D. Varon, "Wave propagation in microstrip transmission lines," presented at the Int. Microwave Symp. (Dallas, TX, May 1969, paper MAM-I-1.

[6] T. Itoh and A. S. Hebert, "A generalized spectral domain analysis for coupled suspended microstrip lines with tuning septums," *IEEE Trans. Microwave Theory Tech.*, vol. MTT-26, pp. 820–826, Oct. 1978.

[7] J. B. Davies and D. Mirshekar-Syahkal, "Spectral domain solution of arbitrary coupled transmission lines with multilayer substrate," *IEEE Trans. Microwave Theory Tech.*, vol. MTT-25, pp. 143–146, Feb. 1977.

[8] P. J. Meier, "Two new integrated circuit media with special advantages of millimeter wavelengths, presented at the 1972 IEEE G-MTT Int. Microwave Symp. (Arlington Heights, IL, May 1972).